Electronic Supplementary Material (ESI) for RSC Advances

A close-up on doxorubicin binding to γ-cyclodextrin: an elucidating spectroscopic, photophysical and conformational study

Resmi Anand, Stefano Ottani, * Francesco Manoli, Ilse Manet, and Sandra Monti *

Istituto per la Sintesi Organica e la Fotoreattività, ISOF-CNR,
via P. Gobetti 101, 40129 Bologna, Italy.

Supplementary Information

(SI-1) Dimerization of DOX

A set of absorption spectra was obtained upon DOX dilution in the range 5.0×10^{-5} M – 1.0×10^{-7} M (Fig. S1). The whole set of spectra was globally analysed adopting a dimerization equilibrium model with the program SPECFIT/32 based on Singular Value Decomposition (SVD) and non linear regression methods (see SI-4 below). According to literature [1, 2] the experimental absorption spectrum at concentration ~ 1×10^{-6} M (λ_{max} = 500 nm, ε ~ 12000 M^{-1} cm^{-1}) was assigned to the monomer. This spectrum was fixed in the calculation. A dimerization constant log (K_d/M^{-1}) = 4.8±0.1 was determined. The spectra of the DOX dimer was also extracted and is reported together with that of monomer in the inset of Fig. S1.

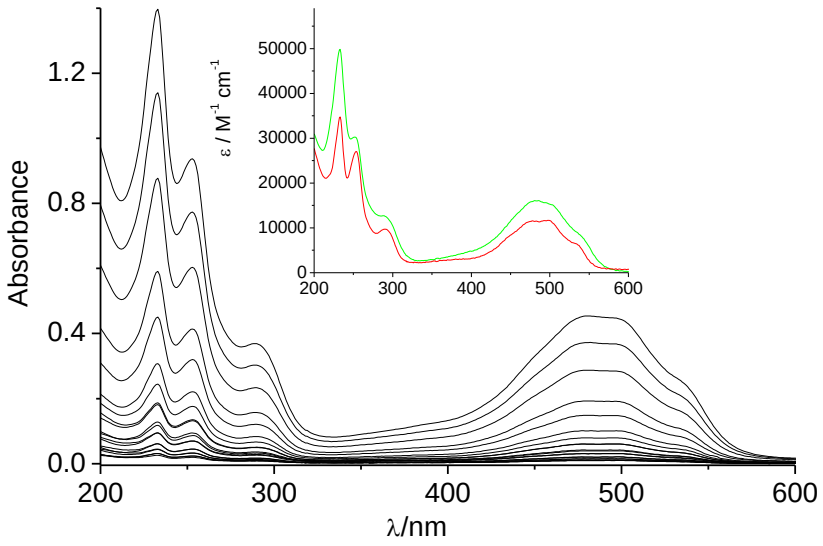

Fig. S1- Absorption spectra upon DOX dilution in the range 5.0×10^{-5} M – 1.0×10^{-7} M, in 0.01 M phosphate buffer at pH 7.4, at 22 °C. Cells of different paths were used to register the spectra that are represented after being normalized to cell path of 1 cm. Inset: absolute spectra of DOX monomer (red) and dimer (green).

(SI-2) Titration of DOX at "high" concentration with γ-CyD monitored with CD and UV-Vis absorption

A 1.6×10^{-4} M solution of DOX in phosphate buffer at pH 7.4 at 22 °C was titrated with γ-CyD from 2.0×10^{-4} M up to 1.6×10^{-2} M. The CD spectra are reported in Figures 1A,B of the main text. A good fit over the whole 200-600 nm range was found for a model with a single 2:2 CyD:DOX complex with an association constant $\log(K_{22}/M^{-3}) = 10.8 \pm 0.2$, Durbin Watson (DW) factor of 1.5 and relative error of fit 3.1% in the 200-280 nm range and DW =1.9 and relative error of fit 6.2% in the 250-600 nm range. The individual spectra of all the species involved in the equilibria are reported in Fig. S2. The agreement between calculated and experimental ellipticities at representative wavelengths is reported in Fig. S3.

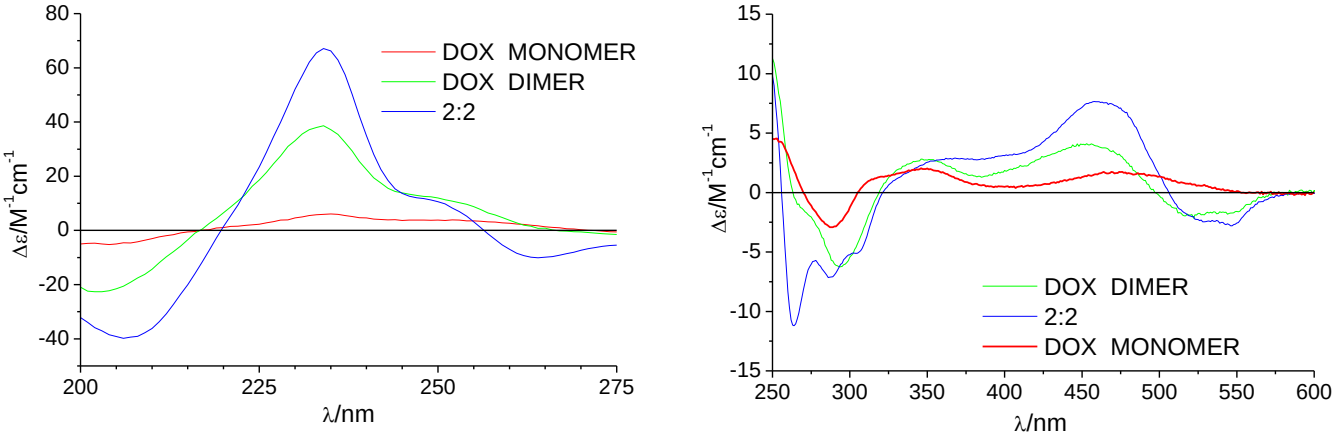

Fig. S2 Absolute spectra of DOX dimer (green) and 2:2 γ-CyD:DOX complex (blue), corresponding to $\log K_d/M^{-1} = 4.8$ and $\log(K_{22}/M^{-3}) = 10.8 \pm 0.2$. The spectrum of free DOX monomer (red) was fixed in the calculations.

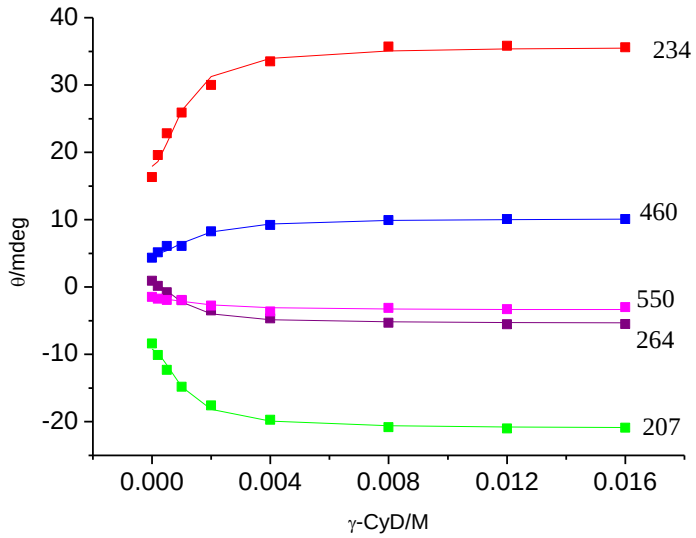

Figure S3. Ellipticity (θ) at key wavelengths of a 1.6×10^{-4} M DOX solution with increasing γ-CyD concentration up to 1.6×10^{-2} M in phosphate buffer 0.01 M of pH 7.4 at 22°C, cell path 0.2 cm below and 0.5 cm above 250 nm. Symbols are experimental values; lines represent best fit values assuming log K_{22}/M^{-3} = 10.7 or 11.0.

The same titration was also followed with UV-vis absorption. Increasing concentrations of γ-CyD cause a 2-3 nm blue-shift of the DOX visible absorption band, small increase of absorbance at 288 nm and 233 nm and small decrease at 252 nm (Fig. S4).

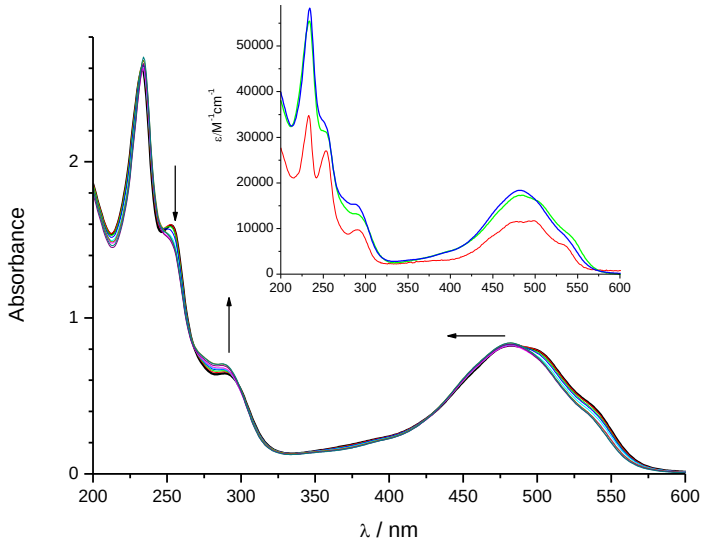

Fig. S4. Absorption spectra of DOX 1.6×10^{-4} M in phosphate buffer at pH 7.4 at 22 °C upon titration with γ-CyD from 2.0×10^{-4} M up to 1.6×10^{-2} M. Cell path 0.5 cm. Inset: absolute spectra of DOX monomer (red); dimer (green); 2:2 γ-CyD:DOX complex (blue).

Global analysis of this set of absorption spectra with the program SPECFIT/32 afforded log(K_{22}/M^{-3}) = 10.8 ± 0.1 (Durbin Watson factor 2.0) in excellent agreement with the result based on CD data (see main text). The spectrum of the DOX monomer was fixed, the spectrum of the 2:2 complex was extracted from the calculation together with that of the DOX dimer (see inset of Fig. S4). The latter agrees fairly well with that reported in the inset of Fig.S1.

In spite of a reasonable agreement of calculated and experimental data with a single 2:2 complex, a better model was found to be that with 1:2 + 2:2 complexes and this latter is described in the main text.

(SI-3) Titration of DOX at "low" concentration with γ-CyD monitored with UV-Vis absorption

A 1.0×10^{-5} M solution of DOX in phosphate buffer at pH 7.4 at 22 °C was titrated with γ-CyD in the range 5.0×10^{-5} M - 1.2×10^{-2} M. Increasing concentrations of γ-CyD cause a slight increase of the absorbance of the visible band with blue-shift of the maximum from 500 to 488 nm and an increase of the absorbance at 288 nm. Only small absorbance changes were observed at 233 nm and 252 nm (Fig. S5). Global analysis was performed with SPECFIT/32 adopting the binding model with 1:1 and 2:1 complexes also applied to CD data analysis (see main text). The binding constant for the 1:1 complex was fixed to log K_{11}/M^{-1} = 2.7 (from CD data analysis) and the spectrum of the free DOX monomer was also fixed (see SI-1). The 2:1 complexation equilibrium constant was optimized and resulted log K_{21}/M^{-1} = 4.9 ±0.4, in good agreement with that from CD data analysis. The absolute absorption spectra of the 1:1 and 2:1 complexes were extracted and are represented in the inset of Fig. S5, together with that of the free DOX monomer. The agreement between calculated and experimental ellipticities at representative wavelengths is reported in Fig. S6.

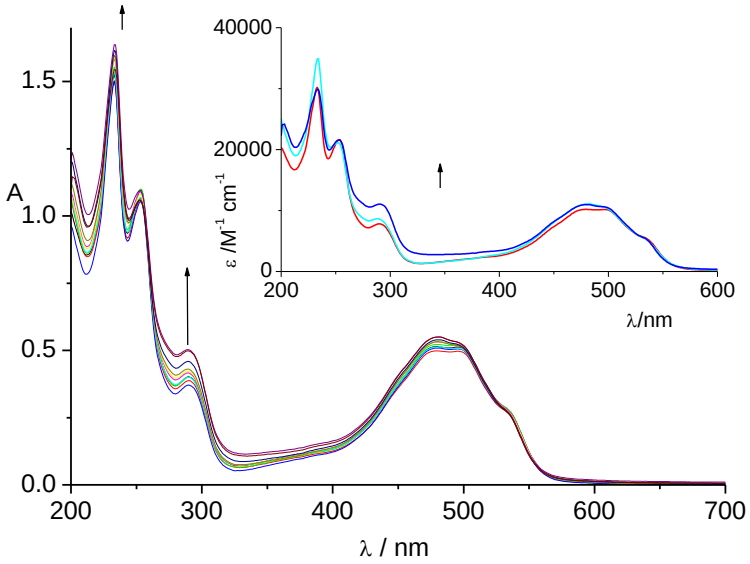

Fig. S5. Absorption spectra of DOX 1.0×10^{-4} M in phosphate buffer at pH 7.4 at 22 °C upon titration with γ-CyD from 5.0×10^{-5} M up to 1.2×10^{-2} M. Cell path 5 cm. Inset: absolute absorption spectra of 1:1 (cyano) and 2:1 (blue) γ-CyD:DOX complexes and DOX monomer (red).

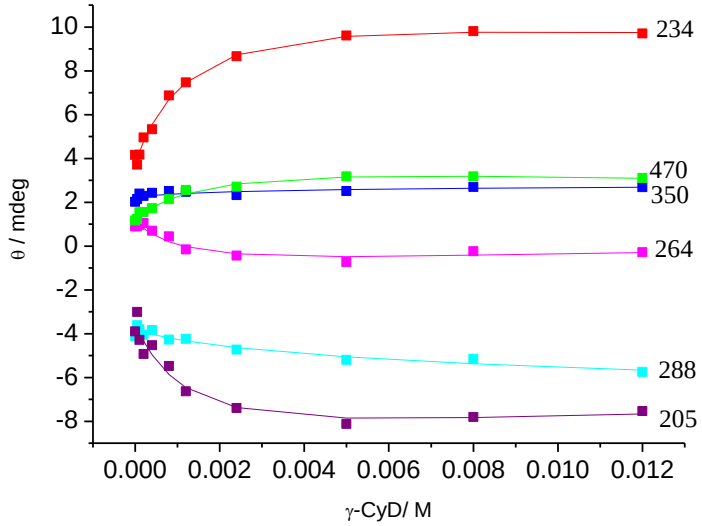

Figure S6. Ellipticity (θ) at key wavelengths of a 1.0×10^{-5} M DOX solution with increasing γ-CyD concentration up to 1.6×10^{-2} M in phosphate buffer 0.01 M of pH 7.4 at 22°C, cell path 2 cm below 250 nm and 4 cm above 250 nm. Symbols are experimental values; lines represent best fit values with log K_{11}/M^{-1} = 2.7 and K_{21}/M^{-2} = 4.4.

(SI-4) Global analysis of equilibrium spectroscopic data with Singular Value Decomposition (SVD) and non linear regression modelling

This application was performed using the commercial SPECFIT/32 program, based on the publications of A. Zuberbühler.[3, 4] Multiwavelength spectroscopic data sets are arranged in matrix form **Y**, where a number Nw of wavelengths and a number Nm of corresponding measured

spectroscopic signals are ordered in columns, whereas ligand and receptor concentrations are inserted in rows. Thus each element of the data matrix Y_{ij} corresponds to a wavelength j and an experimental quantity (absorbance, circular dichroism, fluorescence intensity) for a given couple of concentrations i of ligand and receptor (typically in our experiments one of them is kept constant). A least square best estimator **Y'** of the original data **Y** is reconstructed as the eigenvector representation **Y'** = **U×S×V**, where **S** is a vector that contains the relative weights of the significant eigenvectors (Ne, number of significant eigenvectors), **U** is a matrix (Nm×Ne) of concentration eigenvectors ($U^T \times U=1$, orthonormal) and **V** (Ne×Nw) is a matrix of spectroscopic eigenvectors ($V \times V^T$, orthonormal). This **Y'** matrix contains less noise than **Y** because the SVD procedure can factor random noise from the principal components. This reconstructed data matrix **Y'** is utilized in the global fitting instead of the original data matrix **Y**. Complexation equilibria are solved assuming a complexation model (i.e. contemporary presence of complexes of given stoichiometries in equilibrium with free species in solution) and optimizing the numeric combination of all the spectroscopic contributions to best reproduce the **Y'** signals. Optimization is performed by the nonlinear least square method, using the Levenberg-Marquardt algorithm, for all the explored wavelengths and ligand-receptor concentration couples. The optimized parameters are the association constants. The spectra of the equilibrium components are also extracted from the calculation. The best fits were evaluated on the basis of their Durbin-Watson (DW) factors and the relative error of fit. The DW test is very useful to check for the presence of auto-correlation in the residuals. This method is recommended for systematic misfit errors that can arise in titration experiments. It examines the tendency of successive residual errors to be correlated. The Durbin-Watson statistics ranges from 0.0 to 4.0, with an optimal mid-point value of 2.0 for uncorrelated residuals (i.e., no systematic misfit). In contrast to the χ^2 (Chi-squared) statistics, which requires the noise in the experimental data is random and normally distributed, the DW factor is meaningful even when the noise level in the data set is low. Since the factorized data usually have a significantly lower noise level than the original data, DW test is ideal for the present type of data.

We applied this method to analyze absorption, circular dichroism and fluorescence titration experiments. Below an example of the application is given for the titration of DOX (1.0×10^{-5} M) with γ-CyD with CD monitoring. The SVD analysis of the data in the 250-650 nm range, represented in Figure 3B of the main paper, is the following:

[FACTOR ANALYSIS]
Tolerance = 1.000E-09
Max.Factors = 10
Num.Factors = 5
Significant = 2
Eigen Noise = 3.515E-02
Exp't Noise = 1.406E-01

#	Eigenvalue	Square Sum	Residual	Prediction
1	8.985E+02	2.705E+01	7.832E-02	Data Vector
2	2.160E+01	5.448E+00	3.515E-02	Data Vector
3	2.208E+00	3.239E+00	2.711E-02	Possibly Data
4	1.118E+00	2.121E+00	2.194E-02	Probably Noise
5	3.849E-01	1.736E+00	1.985E-02	Probably Noise

In Figure S6 the agreement between the experimental data and the best fit values at key wavelengths is shown for the model involving DOX monomer in equilibrium with 1:1 and 2:1 γ-CyD:DOX complexes (three principal components), with optimized parameters log K_{11}/M^{-1} = 2.7 ± 0.2 and K_{21}/M^{-2} = 4.4 ± 0.5, Durbin Watson factor 1.7. For the relevant individual spectra of the species in solution, see Fig. 3C,D of main paper.

(SI-5) Distances along the eight MD trajectories and RMSD vs. time.

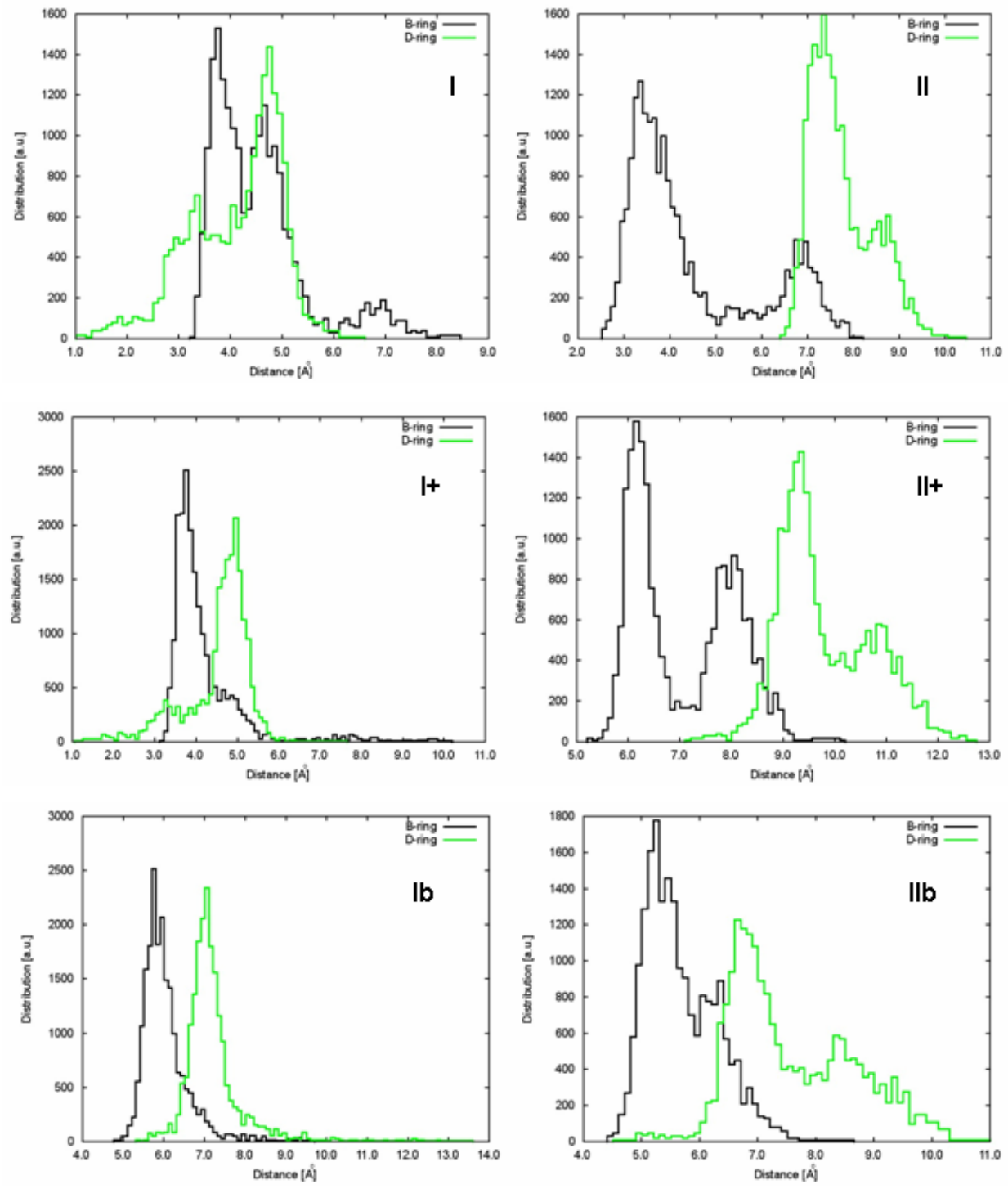

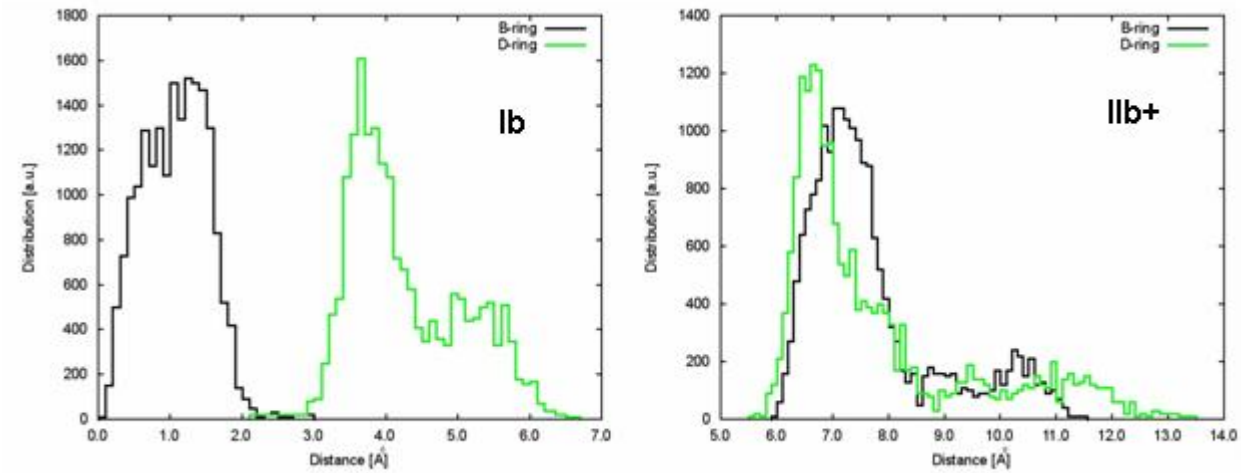

Figure S7. Distribution of distances between the γ-CyD center of mass and the B-ring (black) or the D-ring (green) of the aglycone moiety along the eight MD trajectories.

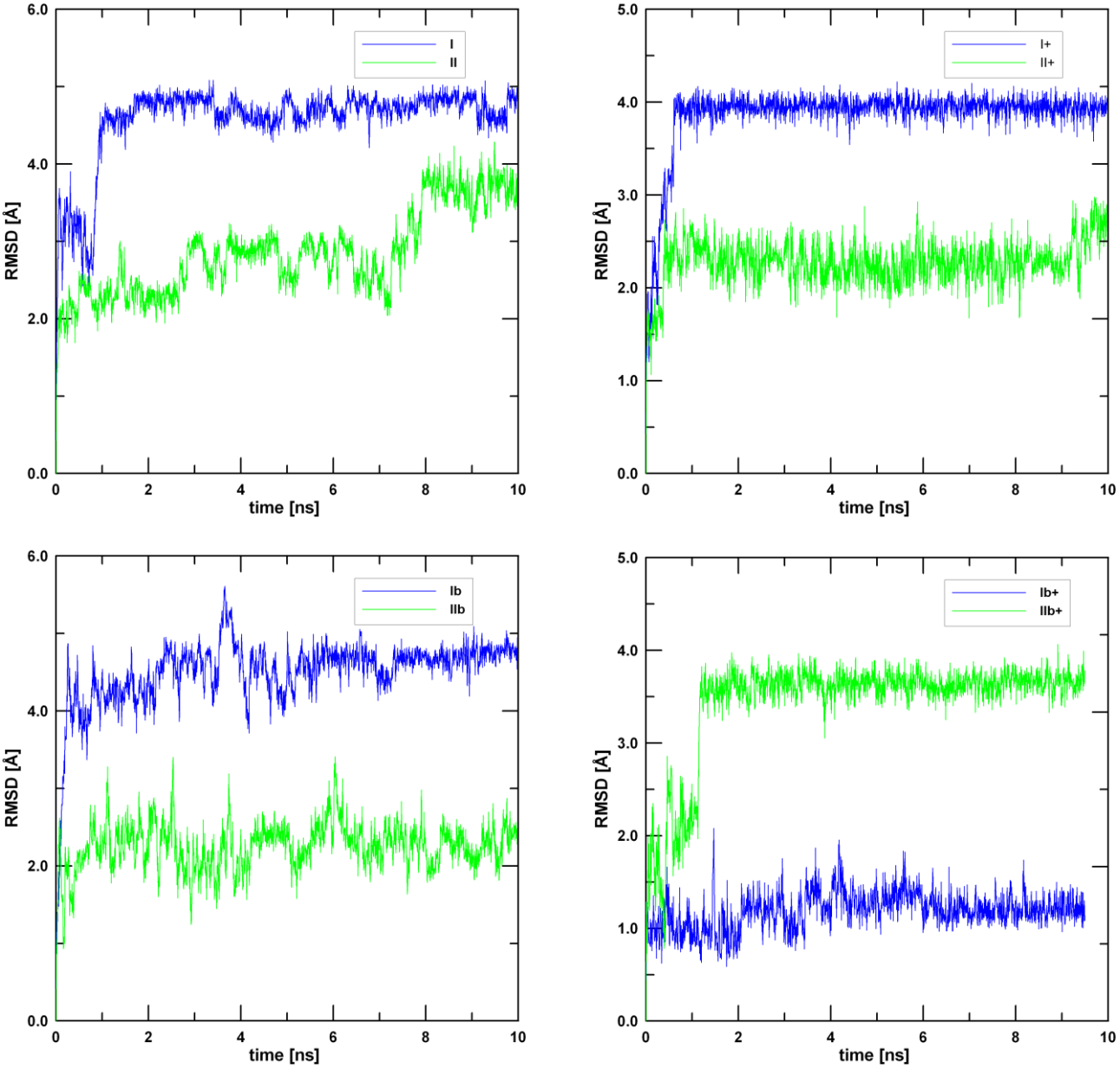

Figure S8. Root Mean Square Deviations (RMSD) *vs* simulation time. Geometries at time 0 are taken as reference to compute RMSD values for each frame along the trajectories.

Table S1: Average value of RMSD (Å) and the corresponding standard deviation for the eight trajectories in Fig. S7. Averages are computed in the interval 1-10ns

I	**II**	**I+**	**II+**	**Ib**	**IIb**	**Ib+**	**IIb+**
1.81±0.25	2.55±0.99	1.07±0.16	1.98±0.73	2.06±0.58	1.69±0..68	1.23±0.24	2.96±0.29

Plots in Fig. S8 and Table S1 show that for times > 1 ns values of RMSD display only minor oscillations around their average values, with the possible exception of RMSDs corresponding to the II initial setting whose deviations are more significant.

Bibliography

1. P. Agrawal, S. K. Barthwal and R. Barthwal, European Journal of Medicinal Chemistry, 2009, 44, 1437-1451.
2. V. Rizzo, C. Battistini, A. Vigevani, N. Sacchi, G. Razzano, F. Arcamone, A. Garbesi, F. Colonna, M. L. Capobianco and L. Tondelli, Journal of Molecular Recognition, 1989, 2, 132-141.
3. H. Gampp, M. Maeder, C. J. Meyer and A. D. Zuberbuhler, Talanta, 1985, 32, 95-101.
4. H. Gampp, M. Maeder, C. J. Meyer and A. D. Zuberbuhler, Talanta, 1985, 32, 257-264.